Acta Crystallographica Section C
Crystal Structure Communications
ISSN 0108-2701

The bis(acetonitrile-κN)bis[*N*,*N*-bis(diphenylphosphanyl)ethanamine-$\kappa^2 P,P'$]iron(II) tetrabromidoferrate(II) and μ-oxido-bis[tribromidoferrate(III)] complex salts

Norah Maithufi[a] and Stefanus Otto[b]*‡

[a]Sasol Technology Research and Development, Department of Chemistry, 1 Klasie Havenga Road, Sasolburg 1947, South Africa, and [b]Department of Chemistry, University of the Free State, PO Box 339, Bloemfontein 9300, South Africa
Correspondence e-mail: fanie.otto@sasol.com

Received 3 May 2011
Accepted 5 July 2011
Online 22 July 2011

Orange crystals of bis(acetonitrile-κN)bis[*N*,*N*-bis(diphenylphosphanyl)ethanamine-$\kappa^2 P,P'$]iron(II) tetrabromidoferrate(II), $[Fe(CH_3CN)_2(C_{26}H_{25}NP_2)_2][FeBr_4]$, (I), and red crystals of bis(acetonitrile-κN)bis[*N*,*N*-bis(diphenylphosphanyl)ethanamine-$\kappa^2 P,P'$]iron(II) μ-oxido-bis[tribromidoferrate(III)], $[Fe(CH_3CN)_2(C_{26}H_{25}NP_2)_2][Fe_2Br_6O]$, (II), were obtained from the same solution after prolonged exposure to atmospheric oxygen, resulting in partial oxidation of the $[FeBr_4]^{2-}$ anion to the $[Br_3FeOFeBr_3]^{2-}$ anion. The asymmetric unit of (I) consists of three independent cations, one on a general position and two on inversion centres, with two anions, required to balance the charge, located on general positions. The asymmetric unit of (II) consists of two independent cations and two anions, all on special positions. The geometric parameters within the coordination environments of the cations do not differ significantly, with the major differences being in the orientation of the phenyl rings on the bidentate phosphane ligand. The ethyl substituent in the cation of (II) and the Br atoms in the anions of (II) are disordered. The P—Fe—P bite angles represent the smallest angles reported to date for octahedral Fe^{II} complexes containing bidentate phosphine ligands with MeCN in the axial positions, ranging from 70.82 (3) to 70.98 (4)°. The average Fe—Br bond distances of 2.46 (2) and 2.36 (2) Å in the $[FeBr_4]^{2-}$ and $[Br_3FeOFeBr_3]^{2-}$ anions, respectively, illustrate the differences in the Fe oxidation states.

Comment

The bis(diphenylphosphanyl)amine ligands (PNP), used together with Cr(acac)$_3$(Hacac is acetylacetone) as the metal source, have been studied extensively and used successfully for selective olefin oligomerization, with high activities and

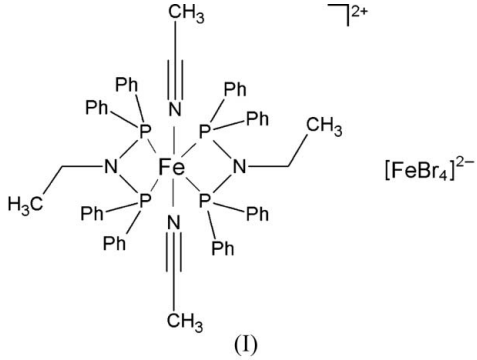

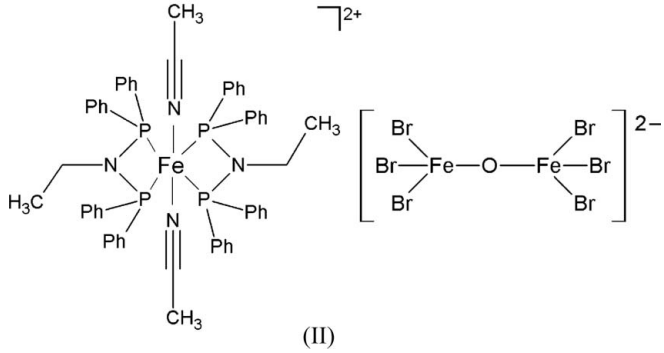

selectivities reported for the trimerization and tetramerization of ethylene (Bollmann *et al.*, 2004; Blann *et al.*, 2005; Overett *et al.*, 2005). As part of our general interest (Maithufi, 2010) in bidentate phosphane ligands containing the PNP bridging unit, we additionally obtained crystals of the two title iron

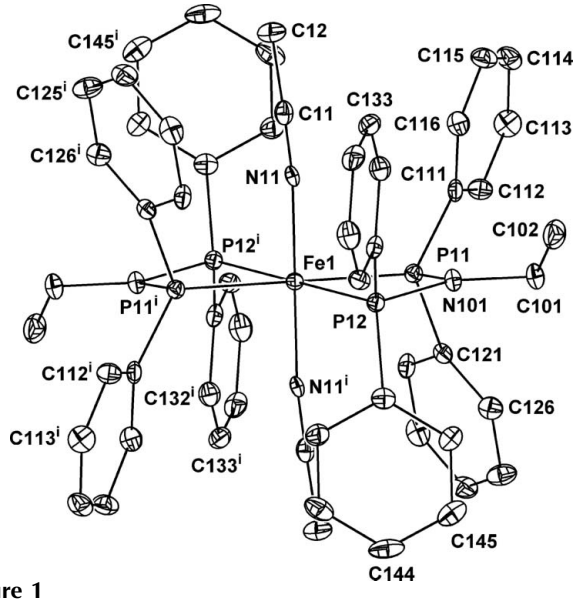

Figure 1
A molecular diagram showing the atom-numbering scheme for cation 1 of (I), situated on an inversion centre. Cation 3 in (I) is also situated on an inversion centre and is numbered accordingly, with the first digit referring to the number of the molecule and the second and third digits referring to the number of the atom in the molecule. Displacement ellipsoids are drawn at the 50% probability level. H atoms have been omitted for clarity. [Symmetry code: (i) $-x$, $-y$, $-z+1$.]

‡ Currently employed at: Sasol Technology Research and Development, 1 Klasie Havenga Road, Sasolburg 1947, South Africa.

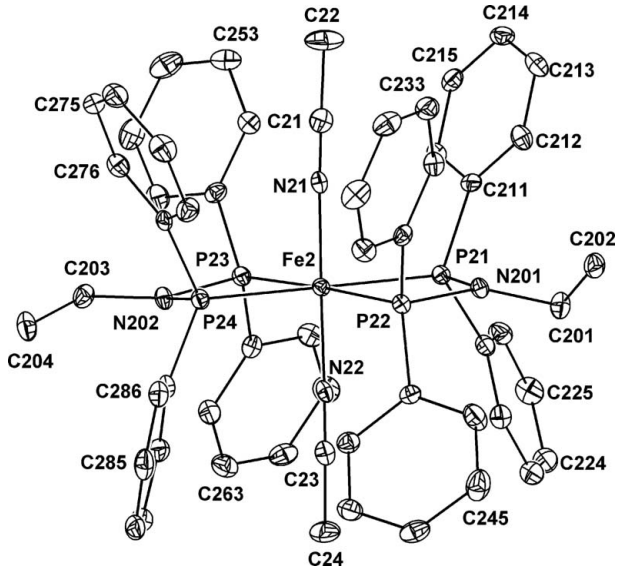

Figure 2
A molecular diagram showing the atom-numbering scheme for cation 2 of (I), situated on a general position. The first digit refers to the number of the molecule, with the second and third digits referring to the number of the atom in the molecule. Displacement ellipsoids are drawn at the 50% probability level. H atoms have been omitted for clarity.

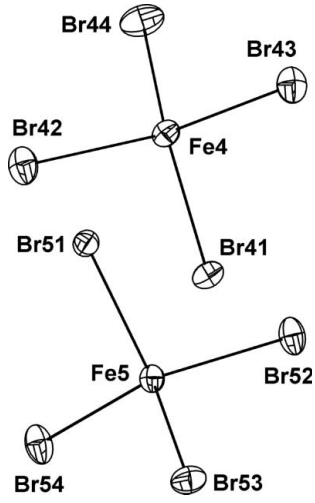

Figure 3
A molecular diagram showing the atom-numbering scheme for the anions in (I). Displacement ellipsoids are drawn at the 50% probability level.

complexes, (I) and (II), the structures of which are reported here.

Upon solving the crystal structures for the two sets of crystals, it was found that the cations in both compounds correspond to $[Fe(MeCN)_2\{Ph_2PN(Et)PPh_2\}_2]^{2+}$, while the anions are different, with $[FeBr_4]^{2-}$ in the orange crystals of (I) and $[Br_3FeOFeBr_3]^{2-}$ in the red crystals of (II). The molecular structures of representative cations and the anions, with the associated numbering schemes, are shown in Figs. 1–5, and selected geometric parameters are presented in Tables 3 and 4 for the cations and anions, respectively.

The chemical formula for (I) was determined to be $[Fe(MeCN)_2\{Ph_2PN(Et)PPh_2\}_2][FeBr_4]$, with three indepen-

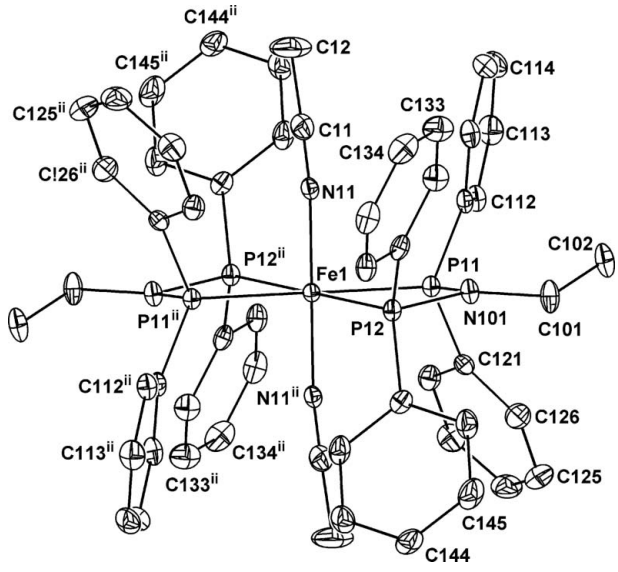

Figure 4
A molecular diagram showing the atom-numbering scheme for cation 1 of (II), situated on an inversion centre. Cation 2, also situated on an inversion centre, is numbered accordingly, with the first digit referring to the number of the molecule and the second and third digits referring to the number of the atom in the molecule. Displacement ellipsoids are drawn at the 50% probability level. H atoms have been omitted for clarity. [Symmetry code: (ii) $-x+1, -y, -z+2$.]

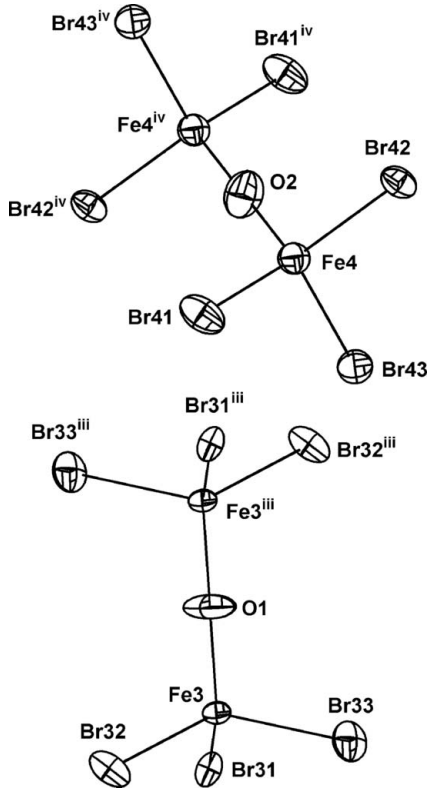

Figure 5
A molecular diagram showing the atom-numbering scheme for the anions in (II). Displacement ellipsoids are drawn at the 50% probability level. The minor-component disordered Br atoms (see *Comment*) have been omitted for clarity. [Symmetry codes: (iii) $-x+1, -y+1, -z+2$; (iv) $-x, -y+1, -z+1$.]

dent cations; cations 1 and 3 are situated on inversion centres, while cation 2 occupies a general position. Both anions, required to balance the charge, are located on general positions. Except for the two coordinated MeCN molecules in each of the cations, no additional solvent molecules were detected in the structure. The cations in (I) are distorted octahedral moieties with two $Ph_2PN(Et)PPh_2$ ligands, each coordinated in a bidentate fashion to the Fe^{II} metal centre, occupying the equatorial plane, and two MeCN molecules in the apical positions (Figs. 1 and 2). Since the $Ph_2PN(Et)PPh_2$ ligands form a four-membered chelate upon coordination, the P—Fe—P angles deviate significantly from the ideal value of 90°, with values ranging from 70.82 (3) to 70.96 (3)° observed in the three crystallographically independent molecules (Table 3). In all cases, one of the Fe—P bond distances is significantly shorter than the other, at *ca* 2.25 Å *versus ca* 2.28 Å, with individual values ranging from 2.2499 (7) to 2.2877 (7) Å. The Fe—N bonds to the acetonitrile are identical at 1.906 (2) Å, while the C—N—Fe angles deviate significantly from 180°, ranging from 171.2 (2) to 176.1 (2)°.

The anions in (I) consist of Fe^{II} cations surrounded by four bromide anions in a distorted tetrahedral arrangement (Fig. 3). As a consequence of their greater degree of freedom, the Fe—Br bond distances vary to a larger degree than the bond distances of equivalent sets of bonds found in the cations. Nevertheless, all distances are still within normal limits for bonds of this nature, ranging from 2.4348 (5) to 2.4948 (5) Å (Mikhailine *et al.*, 2008; Pohl *et al.*, 1995) (Table 4).

The chemical formula for the red crystals, (II), was determined as $[Fe(MeCN)_2\{Ph_2PN(Et)PPh_2\}_2][Br_3FeOFeBr_3]$. The asymmetric unit consists of two independent cations and two $[Br_3FeOFeBr_3]^{2-}$ anions with all moieties situated on special positions. The anions result, presumably, from partial air oxidation of the Fe^{II} used in the synthesis to the Fe^{III} oxidation state associated with this anion. The ethyl substituent in cation 2 is disordered over two positions (see *Experimental*). In addition, the Br atoms in the anions are also disordered over multiple positions (see *Experimental*).

The geometry of the cations in (II) is very similar to that in (I), as shown by the Fe—P bond distances, the average Fe—N bond distances and the average P—Fe—P bite angles (Table 3). Since cations in the two structures are identical, geometric differences are expected to be due to packing effects in the respective crystal structures (Tables 1 and 2). There are significant differences in the orientations of the phenyl rings of the various cations in both structures, as shown by the relevant torsion angles (Table 3). The $[Br_3FeOFeBr_3]^{2-}$ anion in (II) lies across a crystallographic inversion centre and the Fe—O—Fe angle is 180° by symmetry, with each Fe^{III} cation surrounded by three bromide anions to complete a distorted tetrahedral arrangement around Fe. The Fe—O bond distances of 1.7469 (6) and 1.7358 (6) Å indicate the single-order nature of this bond (Table 4). Both the final Fe—Br and Fe—O bond distances are within the typical range for these anions (Evans *et al.*, 1992; Merkel *et al.*, 2005; Busi *et al.*, 2006).

From the data presented in Table 5 for representative $[Fe(MeCN)_2(P–P)_2]^{2+}$ cations, only one other structure was found where the bidentate bisphosphine ligand ($Ph_2PCH_2PPh_2$) forms a four-membered chelate (Gilbertson *et al.*, 2007). The values obtained for the P—Fe—P bite angle of the $Ph_2PN(Et)PPh_2$ ligand, reported in this study, represent the smallest bite angles reported to date for bidentate phosphine ligands in complexes of this nature. The average Fe—P bond distances listed in Table 5 range from 2.259 (2) to 2.340 (1) Å and the values obtained during the current study fall well within this range, despite the P—Fe—P angle deviating significantly from the ideal value of 90° required for optimal orbital overlap. The Fe—N bond distances are in the narrow range 1.889 (11)–1.9188 (19) Å.

Weak intermolecular C—H···Br interactions are present in the two structures (Tables 1 and 2), particularly in (I). In addition, some significant C—H···π interactions of less than 3 Å are also observed; these were evaluated using *PLATON* (Spek, 2009).

The $[FeBr_4]^{2-}$ anion is significantly less common than the Fe^{III} version, $[FeBr_4]^-$. A general search of the Cambridge Structural Database (CSD, Version 5.31, August 2010 update; Allen, 2002) for the $FeBr_4$ fragment (no charge specified) yielded 93 hits, with only five corresponding to Fe^{II}. In addition, this report represents only the fourth crystallographic description of the $[Br_3FeOFeBr_3]^{2-}$ anion found in the open literature. In the Fe^{III} anion, the bond distances are significantly shorter, at 2.24–2.34 Å, and may be used as a basis for distinguishing between the Fe^{II} and Fe^{III} oxidation states in these molecules (Ondrejkovičová & Vrábel, 2002). Here, the average Fe—Br bond distance of 2.364 (14) Å in the $[Br_3FeOFeBr_3]^{2-}$ anion is significantly shorter than the average of 2.4650 (6) Å determined for the Fe—Br bonds for Fe^{II} in $[FeBr_4]^{2-}$, but slightly longer than those found for Fe^{III} in $[FeBr_4]^-$.

Experimental

The $Ph_2PN(Et)PPh_2$ ligand was prepared as described previously (Bollmann *et al.*, 2004), while $FeBr_2$ (98%) and acetonitrile were both purchased from Aldrich and used as received.

The compounds were prepared by dissolving $FeBr_2$ (20 mg, 9.27×10^{-5} mol) and $Ph_2PN(Et)PPh_2$ (38 mg, 9.27×10^{-5} mol) in acetonitrile (10 ml) with stirring under an inert atmosphere. The reaction medium was stirred at room temperature until complete dissolution of the $FeBr_2$ was achieved.

Crystals suitable for X-ray diffraction were obtained by slow evaporation of the acetonitrile solvent from the reaction mixture under aerobic conditions. Visual inspection of the crystals under a microscope indicated the presence of orange and red crystals. Representatives of each colour were selected by hand and used for crystallographic studies. The crystals of (I) were prismatic and orange in colour, while those for (II) were red, slightly larger and with a rectangular cross-section.

^1H and ^{31}P NMR analyses (CD_2Cl_2) of (I) and (II) were identical, with only broad singlets obtained in the ^1H spectra due to the paramagnetic nature of iron. ^1H NMR: δ 0.7–3.2 (12H), 3.6–4.7 (4H), 6.6–7.9 (24H), 7.9–9.9 (16H); ^{31}P NMR: δ 103.83.

Table 1
Hydrogen-bond geometry (Å, °) for (I).

*Cg*14 is the centroid of the C281–C286 ring.

D—H···*A*	*D*—H	H···*A*	*D*···*A*	*D*—H···*A*
C32—H32*B*···Br42^{i}	0.96	2.80	3.718 (3)	160
C315—H315···Br42^{i}	0.93	2.93	3.746 (3)	147
C276—H276···Br44	0.93	2.93	3.607 (3)	131
C202—H20*E*···Br41^{ii}	0.96	2.83	3.741 (3)	159
C225—H225···Br51^{iii}	0.93	2.77	3.658 (3)	159
C262—H262···Br51	0.93	2.88	3.540 (3)	129
C326—H326···Br51	0.93	2.89	3.571 (3)	131
C12—H12*B*···Br52	0.96	2.83	3.724 (3)	154
C201—H20*A*···Br53^{iv}	0.97	2.86	3.762 (3)	155
C24—H24*A*···Br53	0.96	2.92	3.755 (3)	146
C242—H242···*Cg*14	0.93	2.78	3.553 (3)	142

Symmetry codes: (i) $-x, -y+1, -z+1$; (ii) $-x+1, -y+1, -z$; (iii) $x+1, y, z$; (iv) $-x+1, -y, -z$.

Compound (I)

Crystal data

$[Fe(C_2H_3N)_2(C_{26}H_{25}NP_2)_2][FeBr_4]$
M_r = 1340.27
Triclinic, $P\overline{1}$
a = 11.4596 (10) Å
b = 21.834 (2) Å
c = 23.905 (2) Å
α = 114.399 (1)°
β = 96.285 (1)°
γ = 90.388 (1)°
V = 5405.4 (8) Å^3
Z = 4
Mo $K\alpha$ radiation
μ = 3.65 mm^{-1}
T = 100 K
0.40 × 0.20 × 0.08 mm

Data collection

Bruker APEX CCD area-detector diffractometer
Absorption correction: multi-scan (*SADABS*; Bruker, 2009)
T_{min} = 0.323, T_{max} = 0.771
59375 measured reflections
21891 independent reflections
16724 reflections with $I > 2\sigma(I)$
R_{int} = 0.038

Refinement

$R[F^2 > 2\sigma(F^2)]$ = 0.033
$wR(F^2)$ = 0.074
S = 1.00
21891 reflections
1272 parameters
H-atom parameters constrained
$\Delta\rho_{max}$ = 0.61 e Å^{-3}
$\Delta\rho_{min}$ = −0.41 e Å^{-3}

Compound (II)

Crystal data

$[Fe(C_2H_3N)_2(C_{26}H_{25}NP_2)_2]$-$[Fe_2Br_6O]$
M_r = 1571.94
Monoclinic, $P2_1/c$
a = 18.928 (5) Å
b = 18.352 (4) Å
c = 17.243 (4) Å
β = 90.365 (3)°
V = 5989 (3) Å^3
Z = 4
Mo $K\alpha$ radiation
μ = 4.87 mm^{-1}
T = 100 K
0.55 × 0.24 × 0.22 mm

Data collection

Bruker APEXII CCD area-detector diffractometer
Absorption correction: multi-scan (*SADABS*; Bruker, 2009)
T_{min} = 0.175, T_{max} = 0.413
64539 measured reflections
13071 independent reflections
10694 reflections with $I > 2\sigma(I)$
R_{int} = 0.038

Refinement

$R[F^2 > 2\sigma(F^2)]$ = 0.039
$wR(F^2)$ = 0.097
S = 1.04
13071 reflections
758 parameters
49 restraints
H-atom parameters constrained
$\Delta\rho_{max}$ = 3.18 e Å^{-3}
$\Delta\rho_{min}$ = −1.08 e Å^{-3}

Table 2
Hydrogen-bond geometry (Å, °) for (II).

*Cg*11 is the centroid of the C111–C116 ring and *Cg*10 is the centroid of the C131–C136 ring.

D—H···*A*	*D*—H	H···*A*	*D*···*A*	*D*—H···*A*
C22—H22*B*···Br43 (major site)	0.96	2.75	3.653 (5)	157
C142—H142···*Cg*11^{i}	0.93	2.73	3.517 (4)	143
C214—H214···*Cg*10	0.93	2.73	3.571 (4)	151

Symmetry code: (i) $-x+1, -y+1, -z+1$.

Table 3
Selected geometric parameters (Å, °) for the cations in (I) and (II).

Bond/angle	(I), *n* = 1	(I), *n* = 2	(I), *n* = 3	(II), *n* = 1	(II), *n* = 2
Fe*n*—N*n*1	1.906 (2)	1.906 (2)	1.908 (2)	1.895 (3)	1.901 (3)
Fe*n*—P*n*1	2.2499 (7)	2.2547 (8)	2.2877 (7)	2.2620 (9)	2.2715 (9)
Fe*n*—P*n*2	2.2870 (7)	2.2842 (8)	2.2588 (7)	2.2824 (9)	2.2866 (9)
P*n*1—N*n*01	1.701 (2)	1.696 (2)	1.707 (2)	1.703 (3)	1.699 (3)
P*n*1—Fe*n*—P*n*2	70.82 (3)	70.85 (3)	70.96 (3)	70.97 (3)	70.98 (4)
P21—Fe2—P23		108.97 (3)			
P21—Fe2—P24		179.79 (4)			
P22—Fe2—P23		177.23 (3)			
P22—Fe2—P24		109.36 (3)			
Fe*n*—P*n*1—C*n*11—C*n*12	−116.7 (2)	−109.0 (2)	−130.0 (2)	−106.4 (3)	−121.4 (3)
Fe*n*—P*n*1—C*n*21—C*n*22	64.9 (2)	67.9 (2)	58.2 (2)	64.6 (3)	70.7 (3)
Fe*n*—P*n*2—C*n*31—C*n*32	−54.0 (2)	71.8 (2)	−53.1 (2)	−74.8 (3)	−38.9 (4)
Fe*n*—P*n*2—C*n*41—C*n*42	−55.8 (2)	28.5 (3)	−65.9 (2)	−30.1 (3)	−59.9 (3)

Symmetry code: (i) $-x, -y, 1-z$.

Table 4
Selected bond distances (Å) for the anions in (I) and (II)†.

Bond/angle	(I), *n* = 4	(I), *n* = 5	(II), *n* = 3	(II), *n* = 4
Fe*n*—Br*n*1	2.4583 (5)	2.4716 (5)	2.3814 (8)	2.3703 (9)
Fe*n*—Br*n*2	2.4701 (5)	2.4614 (5)	2.364 (5)	2.3782 (8)
Fe*n*—Br*n*3	2.4948 (5)	2.4485 (5)	2.341 (8)	2.3604 (14)
Fe*n*—Br*n*4	2.4348 (5)	2.4805 (5)		
Fe*n*—O1/O2			1.7469 (6)	1.7358 (6)

† Only the Fe—Br bonds involving the highest-occupancy disordered Br atoms are given (see *Comment*).

The intensity data (2450 frames) were collected with an exposure time of 8 s per frame (frame width = 0.30°) for (I) and 5 s per frame for (II). All non-methyl H atoms were placed in geometrically idealized positions, with C—H = 0.93 Å for CH (aryl) and 0.97 Å for CH_2, and constrained to ride on their parent atoms, with U_{iso}(H) = 1.2U_{eq}(C). The methyl H atoms were constrained to an ideal geometry, with C—H = 0.96 Å and U_{iso}(H) = 1.5U_{eq}(C), but were allowed to rotate freely about the adjacent C—C bond.

The disorder of the ethyl C atoms in cation 2 of (II) was modelled over two sites, with the occupancies initially as free variables summing to unity. Values of 0.511 (14) and 0.489 (14) were obtained, and since these values do not differ significantly from 0.5 they were subsequently fixed at 0.5 for the final refinement. The disorder of the Br atoms in the anions of (II) was modelled using a combination of geometric (all Fe—Br distances) and ellipsoid restraints (similar U^{ij} components). For the Fe4-based anion, two major/minor site occu-

Table 5
Comparative X-ray data for some $[Fe(MeCN)_2(P–P)_2]$ complexes†.

P—P	Fe—P (Å)	P—Fe—P (°)	Fe—N (Å)	Reference
$Me_2P(CH_2)_2PMe_2$	2.267 (4)	84.8 (2)	1.905 (7)	*a*
$Me_2P(CH_2)_2PMe_2$	2.259 (2)	85.17 (6)	1.917 (5)	*b*
$Et_2P(CH_2)_2PEt_2$	2.2784 (11)	84.88 (3)	1.896 (2)	*c*
$Ph_2P(CH_2)_2PPh_2$	2.33 (6)	83.20 (4)	1.91 (10)	*d*
$Ph_2P(CH{=}CH)PPh_2$	2.321 (3)	82.57 (9)	1.916 (10)	*e*
$\{MeO(CH_2)_3\}_2P(CH_2)_2$-$P\{(CH_2)_3OMe\}_2$	2.2926 (6)	84.26 (2)	1.9188 (19)	*f*
$\{HO(CH_2)_3\}_2P(CH_2)_2$-$P\{(CH_2)_3OH\}_2$	2.2967 (4)	84.187 (16)	1.9077 (14)	*g*
$Ph_2P(C_6H_4)PPh_2$	2.340 (1)	81.1 (1)	1.894 (4)	*h*
$Ph_2P(CH_2)PPh_2$	2.275 (6)	73.1 (2)	1.889 (11)	*i*
$Ph_2PN(Et)PPh_2$	2.2715 (8)	70.86 (3)	1.906 (2)	*j*
$Ph_2PN(Et)PPh_2$	2.2757 (9)	70.98 (4)	1.898 (3)	*k*

† Since all the P—P ligands are symmetrical, only average Fe—P bond distances are reported in all cases. References: (*a*) Barron *et al.* (1987); (*b*) George *et al.* (1997); (*c*) Martins *et al.* (1998); (*d*) Blake *et al.* (1992); (*e*) Williams (1988); (*f*) Gilbertson *et al.* (2007); (*g*) Gohdes *et al.* (2009); (*h*) Barclay *et al.* (1988); (*i*) Bechlars *et al.* (2008); (*j*) this work, (I); (*k*) this work, (II).

pancies (summing to 1.0) sufficed, but the disorder at the Fe3-based anion could only be modelled with multiple sites. No evidence was found to suggest that a mixture of anions, such as $[FeBr_4]^{2-}$, exists in this structure.

The minimum and maximum residual electron densities for (II) are located 0.61 Å from Br43 and 1.2 Å from Br46, respectively. The location of the maximum residual electron-density peak does not fit the geometry of any expected disorder or impurity.

For both compounds, data collection: *APEX2* (Bruker, 2009); cell refinement: *SAINT* (Bruker, 2009); data reduction: *SAINT*; program(s) used to solve structure: *SHELXS97* (Sheldrick, 2008); program(s) used to refine structure: *SHELXL97* (Sheldrick, 2008); molecular graphics: *DIAMOND* (Brandenburg & Berndt, 1999); software used to prepare material for publication: *SHELXL97*.

Financial support from Sasol Technology Research and Development and the Research Funds of the University of the Free State is gratefully acknowledged. The Sasol Technology R&D Ligand Synthesis group is thanked for a kind donation of the ligand used in this study. Dr J. A. Gertenbach of the University of Stellenbosch is gratefully acknowledged for the collection of the diffraction data. Dr Alfred Muller of the University of Johannesburg is thanked for valuable assistance with the evaluation of the intermolecular interactions using *PLATON*. Part of this material is based on work supported by the South African National Research Foundation (NRF) under grant No. GUN 2053397. Any opinion, finding and conclusions or recommendations in this material are those of the authors and do not necessarily reflect the views of the NRF.

Supplementary data for this paper are available from the IUCr electronic archives (Reference: GA3164). Services for accessing these data are described at the back of the journal.

References

Allen, F. H. (2002). *Acta Cryst.* B**58**, 380–388.
Barclay, J. E., Hills, A., Hughes, D. L. & Leigh, G. L. (1988). *J. Chem. Soc. Dalton Trans.* pp. 2871–2877.
Barron, A. R., Wilkinson, G., Motevalli, M. & Hursthouse, M. B. (1987). *Polyhedron*, **6**, 1089–1095.
Bechlars, B., Issac, I., Feuerhake, R., Clerac, R., Fuhr, O. & Fenske, D. (2008). *Eur. J. Inorg. Chem.* **10**, 1632–1644.
Blake, A. J., Atkins, A. J., Gould, R. O. & Schroder, M. (1992). *Z. Kristallogr.* **198**, 287–289.
Blann, K., Bollmann, A., Dixon, J. T., Hess, F. H., Killian, E., Maumela, H., Morgan, D. H., Neveling, A., Otto, S. & Overett, M. J. (2005). *Chem. Commun.* pp. 620–621.
Bollmann, A., Blann, K., Dixon, J. T., Hess, F. H., Killian, E., Maumela, H., McGuiness, D. S., Morgan, D. H., Neveling, A., Otto, S., Overett, M. J., Slawin, A. M. Z., Wassercheid, P. & Kuhlmann, S. (2004). *Chem. Commun.* pp. 14712–14713.
Brandenburg, K. & Berndt, M. (1999). *DIAMOND*. Version 2.1a. Crystal Impact GbR, Bonn, Germany.
Bruker (2009). *APEX2*, *SAINT* and *SADABS*. Bruker AXS Inc., Madison, Wisconsin, USA.
Busi, S., Lahtinen, M., Sillanpää, R. & Rissanen, K. (2006). *Acta Cryst.* C**62**, m458–m460.
Evans, P. J. M., Fitzsimmons, B. W., Marshall, W. G., Golder, A. J., Larkworthy, L. F. & Smith, G. W. (1992). *J. Chem. Soc. Dalton Trans.* pp. 1065–1068.
George, A. V., Field, L. D., Malouf, E. Y., McQueen, A. E. D., Pike, S. R., Purches, G. R., Hambley, T. W., Uys, I. E., White, A. H., Hockless, D. C. R. & Skelton, B. W. (1997). *J. Organomet. Chem.* **538**, 101–110.
Gilbertson, J. D., Szymczak, N. K., Crossland, J. L., Miller, W. K., Lyon, D. K., Foxman, J. & Tyler, D. R. (2007). *Inorg. Chem.* **46**, 1205–1214.
Gohdes, J. W., Zakharov, L. N. & Tyler, D. R. (2009). *Acta Cryst.* E**65**, m776.
Maithufi, M. N. (2010). PhD thesis, Technische Universiteit Eindhoven, The Netherlands.
Martins, L. M. D. R. S., Duarte, M. T., Galvao, A. M., Resende, C., Pombeiro, A. J. L., Henderson, R. A. & Evans, D. J. (1998). *J. Chem. Soc. Dalton Trans.* pp. 3311–3318.
Merkel, M., Pascally, M., Krebs, B., Astner, J., Foxon, S. P. & Schindler, S. (2005). *Inorg. Chem.* **44**, 7582–7589.
Mikhailine, A. A., Kim, E., Dingels, C., Lough, A. J. & Morris, R. H. (2008). *Inorg. Chem.* **47**, 6587–6589.
Ondrejkovičová, I. & Vrábel, V. (2002). *J. Coord. Chem.* **55**, 335–343.
Overett, M. J., Blann, K., Bollmann, A., Dixon, J. T., Hess, F. H., Killian, E., Maumela, H., Morgan, D. H., Neveling, A. & Otto, S. (2005). *Chem. Commun.* pp. 622–624.
Pohl, W., Lorenz, I.-P., Noth, H. & Schmidt, M. (1995). *Z. Naturforsch. Teil B*, **50**, 1485–1493.
Sheldrick, G. M. (2008). *Acta Cryst.* A**64**, 112–122.
Spek, A. L. (2009). *Acta Cryst.* D**65**, 148–155.
Williams, A. F. (1988). *Acta Cryst.* C**44**, 1895–1897.